

Sigma Limiting Effects on the Response of a Ceramic Matrix Beam

Howard F. Wolfe,* Michael P. Camden,[†] Dansen L. Brown,[‡] and Larry W. Simmons[§]
U.S. Air Force Research Laboratory, Wright-Patterson Air Force Base 45433-7006

High sigma events were studied in the narrowband random response of a cantilevered beam excited by an electrodynamic shaker. The effects of truncating the input signal to the shaker with a BlackglasTM beam are discussed. Tests were conducted with the shaker option of the shaker controller sigma limiting turned off, sigma limited to 2.5, and sigma limited to 3.5. Large data files were recorded and analyzed. The results were compared with similar previous tests with an aluminum alloy beam. The sigma values calculated varied considerably with the record lengths. When a fatigue failure was assumed, the cumulative fatigue damage was computed as a function of the sigma value of the response peak probability density function. Very little damage was found for the high sigma peaks compared to the damage that occurred with the many smaller peaks.

Introduction

SHAKER tests are used to simulate flight vibration environments to qualify structures and equipment for various aircraft vibration mission requirements. Structural random fatigue life tests are usually performed to qualify structures for the extreme environments of combined high-intensity random noise and high temperatures. Additionally, they are conducted to provide data needed for the prediction of fatigue lifetimes of structural materials and joints of interest. Two types of testing apparatus are commonly used for this purpose. These are the electrodynamic shaker and the acoustic plane progressive wave tubes. Both testing methods offer some degree of control of the peak and amplitude probability density functions. The ability to achieve an environment in the laboratory that duplicates that experienced in flight is not fully understood. The output of many electrodynamic shaker controllers is fixed at a single sigma value, with three sigma being the industry standard. The controller used in these tests permitted the selection of the sigma value as part of the input to the shaker.

Experiments

The effects of varying the spectrum controller's sigma limiting value on the response of a cantilevered beam at room temperature were studied. The effects of the record length in determining high sigma values were studied. The record length of many dynamic tests is rather short in duration and is usually truncated after 5–30 s. This is usually the case for well-established sinusoidal and stationary random data. The record length is kept short for practical reasons, such as minimizing the record storage space and processor size. However, even if random data are considered stationary, the detection of 5 or 6 sigma peaks with a frequency of 300 Hz, for example, would take many hours of recording time to capture 5–6 sigma events. The

record lengths involved require approximately 8 GB of storage space for a single, four-channel record plus the capability of processing the huge data files and presenting the results.

A 4000-lb electrodynamic shaker was used for these tests. The test structure was a cantilevered beam structure with a one-half sine wave clamping arrangement shown in Figs. 1 and 2. An accelerometer was mounted on the shaker head to measure the input acceleration and provide vibration feedback control. Displacements were measured with a laser scanning vibrometer. The vibrometer velocity signal was integrated to yield displacement with an electronic integrator. A low test level was selected to prevent fatigue damage from affecting the long-duration test records. Three narrowband random response tests were conducted at a constant gravitational acceleration root-mean-square (rms) level, each with a different sigma limiting value entered in the controller. The shaker acceleration peak probability density functions (PPDFs) were truncated by using the sigma limiting feature of the shaker controller. The three sigma limiting values were off (none), 2.5, and 3.5. The spectrum controller was programmed for a flat narrowband random accelerometer spectral density shape from 174 to 258 Hz to envelop the bending mode of the test beam. The drive signal to the shaker, the signal from the accelerometer on the shaker table, two strain gauges, and the laser vibrometer were recorded. The center strain gauge was in the center of the beam next to the peak of the sine wave clamp. The side strain gauge (Fig. 1) was located half of the distance from the center of the beam and center on a line tangent to the sine wave clamp. During each response test, four 4200-s recordings were made on a personal computer with a sampling rate of 6000 samples per second.

Results

The first bending mode of the test coupon (222 Hz) was the only modal response frequency present within the excitation frequency range. The narrowband excitation frequency range of 174–258 Hz included this frequency. The time into the record for the highest sigma was found by setting a high exceedance level in the analysis software to find high peaks. A typical response waveform of the accelerometer is shown in Fig. 3.

Typical response waveforms rms of the strain signals that follow those of the displacement are signals shown in Figs. 4 and 5. In this example, the highest acceleration (input) does not occur at the same time as the highest response (output) signal. After examining hundreds of time histories, this was usually found to be the case. The amplitude of the response was not found to be directly related to the input. Figures 6–8 show the timescale expanded from 3629.70 to 3629.90 s. Figures 6–8 illustrate the point that the highest response occurs at 3629.82 s while the excitation level was considerably less than the maximum. The highest acceleration level occurred at 3629.74 s. A short burst of high level excitation builds

Presented as Paper 99-1456 at the 40th Structures, Structural Dynamics, and Materials Conference, St. Louis, MO, 12–15 April 1999; received 14 September 1999; revision received 16 March 2001; accepted for publication 13 April 2001. This material is declared a work of the U.S. Government and is not subject to copyright protection in the United States. Copies of this paper may be made for personal or internal use, on condition that the copier pay the \$10.00 per-copy fee to the Copyright Clearance Center, Inc., 222 Rosewood Drive, Danvers, MA 01923; include the code 0021-8690/02 \$10.00 in correspondence with the CCC.

*Senior Research Engineer, Structures Division, Air Vehicles Directorate, 2145 Fifth Street, Suite 5.

[†]Aerospace Engineer, Structures Division, Air Vehicles Directorate, 2145 Fifth Street, Suite 5.

[‡]Structures Division, Air Vehicles Directorate, 2145 Fifth Street, Suite 5.

[§]Engineering Technician, Structures Division, Air Vehicles Directorate, 2145 Fifth Street, Suite 5.

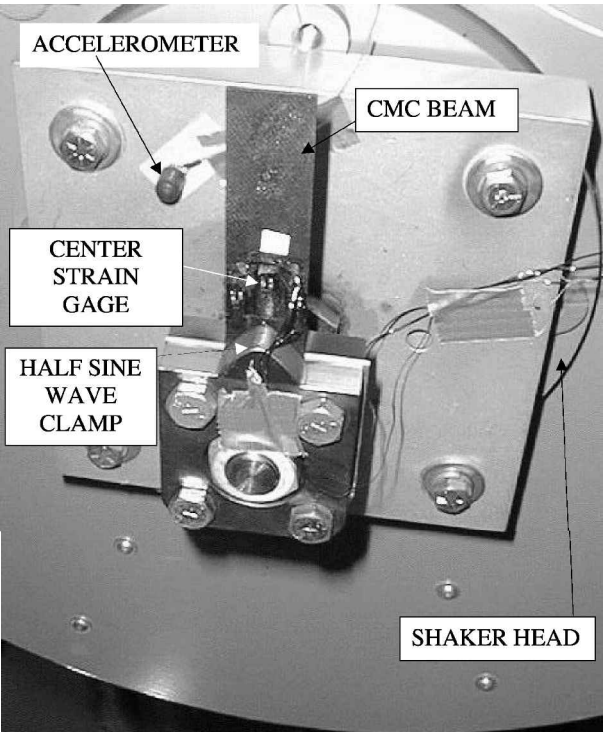


Fig. 1 Blackglas cantilever beam clamping arrangement.

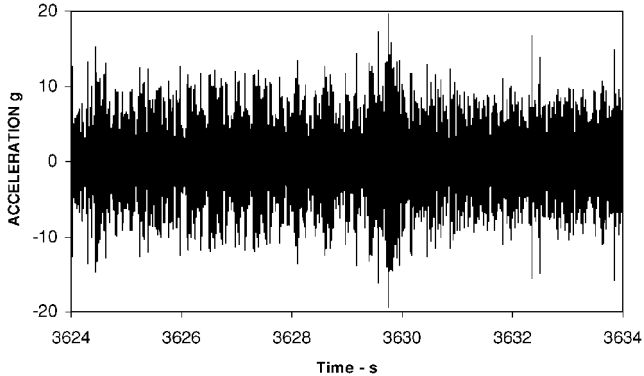


Fig. 3 Acceleration (g) time history, 3624-3634 s.

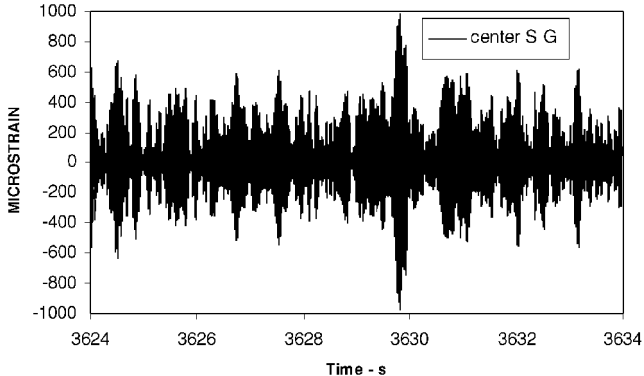


Fig. 4 Center strain gauge (microstrain) time history, 3624-3634 s.

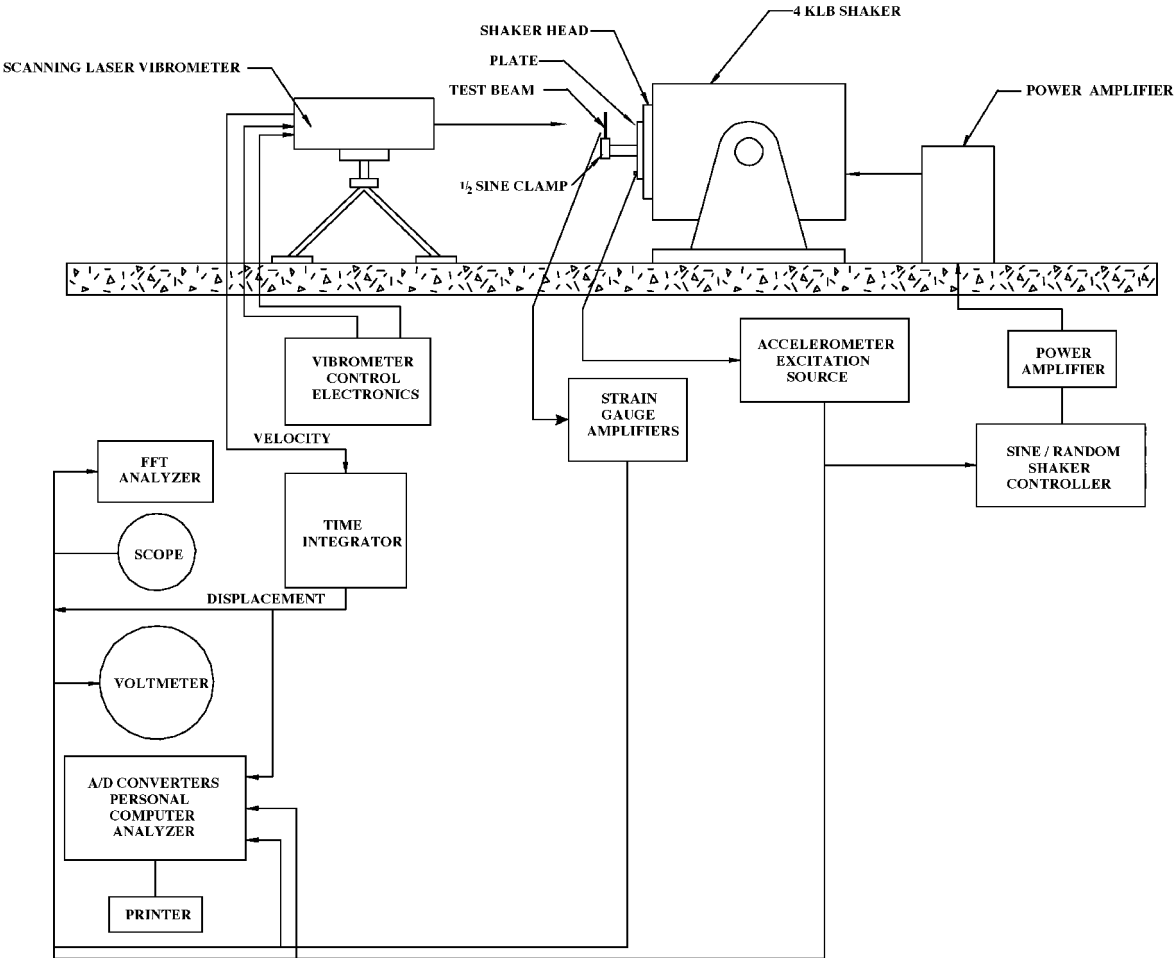
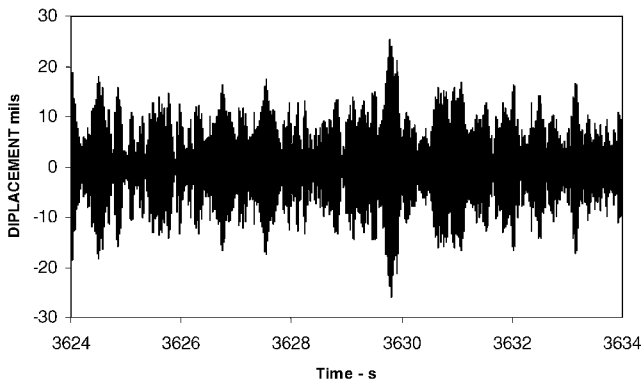
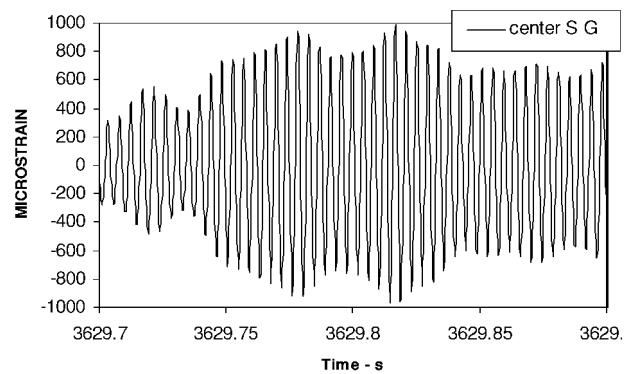
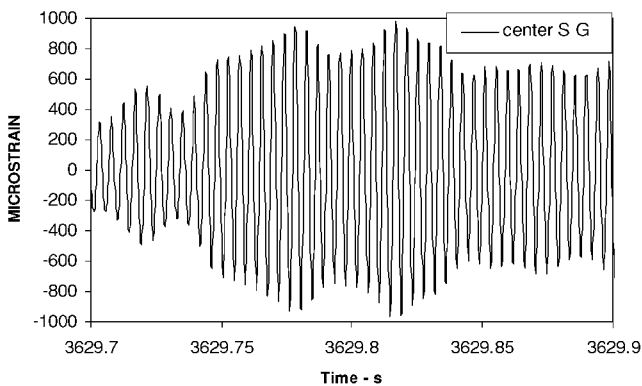
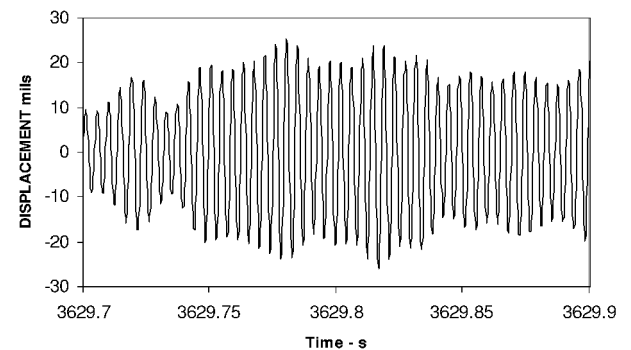


Fig. 2 Blackglas cantilevered beam test setup.

Table 1 Summary of acceleration response

Sigma value	Positive	Negative	Positive	Negative	Positive	Negative	Positive	Negative	Positive	Negative
Sigma off	R 1		R 2		R 3		R 4		R 1–4	
Time, s	2200.52		2317.10		3028.40		1396.93			
Acceleration, g	21.1	–21.5	21.2	–21.2	20.0	–20.0	19.7	–19.4	21.2	–21.5
Calculated	5.40	–5.50	5.28	–5.28	5.12	–5.12	5.03	–4.95	5.41	–5.48
3.5 Sigma	R 5		R 6		R 7		R 8		R 5–8	
Time, s	2268.30		2635.50		3088.60		3942.09			
Acceleration, g	14.0	–13.7	14.0	–13.7	14.3	–14.0	14.3	–14.3	14.3	–14.3
Calculated	3.59	–3.51	3.60	–3.52	3.68	–3.60	3.63	–3.63	3.65	–3.65
2.5 Sigma	R 9		R 10		R 11		R 12		R 9–12	
Time, s	1165.15		3197.77	3550.80	4424.90		2184.66	9206.10		
Acceleration, g	11.0	–11.0	11.0	–10.7	11.0	–11.0	11.0	–11.0	11.0	–11.0
Calculated	2.81	–2.81	2.81	–2.74	2.79	–2.79	2.79	–2.79	28.0	–2.80

**Fig. 5** Displacement (mils) time history, 3624–3634 s.**Fig. 7** Center strain gauge (microstrain) time history, 3629.70–3629.90 s.**Fig. 6** Acceleration (g) time history, 3629.70–3629.90 s.**Fig. 8** Displacement (mils) time history, 3629.70–3629.90 s.

up the response before the amplitude can decay. This phenomenon for a single-mode response is due to the damping in the structure, which results in successive peaks building in amplitude upon previous peaks that have not decayed significantly.

The amplitude probability density functions (APDFs) and PPDFs were calculated from the time histories of the excitation signals and the strain and vibrometer signals. The sigma values were computed by dividing the amplitudes from the APDFs and the peaks from the PPDFs by the standard deviation (SD) rather than the rms value. This method incorporates the nonzero mean values.

The next two paragraphs discuss APDFs. The highest and lowest sigma values obtained from the accelerometer APDFs are listed in Table 1 for each of the four 4200-s records and for the combined 16,800-s records. The largest positive peak was 5.41 from the combination record, and the largest negative peak was –5.50 from the first record. The variations in the sigma values are due to two factors. These factors are the maximum and minimum amplitudes of the 4200-s time histories and the standard deviation for the time sample. The combination values do not always contain the maximum and minimum sigma values because the SDs with all of the peaks were recomputed for the combination. This was

also true with the drive, strain gauge and vibrometer records. The standard deviation may or may not be the largest value for the combination than that of each of the 4200-s components. The maximum SD for the accelerometer was –21.5-g peak from the first record. The clipping reduced the acceleration peak values. With the sigma limited to 2.5, the maximum and minimum peaks were 2.81 and –2.81 for all of the records. The variability was limited to a range of positive values from 2.79 to 2.81 and negative values from –2.74 to –2.81. Much less variability was observed with the clipped tests than the unclipped test. Similar results were obtained with the drive signals with similar variability among the individual records and the combined records. The highest sigma values with the drive signal did not always occur at the same time into the accelerometer record. The drive and accelerometer APDFs are shown in Fig. 9. Both were shaped similar to a Gaussian distribution. The drive signal PPDFs plotted on a logarithm scale for the cases with sigma limiting turned off were nearly the same. The lowest sigma value was –5.40 sigma and the highest was 5.05. This is shown in Figs. 10 and 11. The sigma values near the tails or ends of the curves were slightly larger for the drive signal than for the accelerometer signal.

Table 2 Summary of strain response, center gauge^a

Sigma value	Positive	Negative	Positive	Negative	Positive	Negative	Positive	Negative	Positive	Negative
Sigma off	R 1		R 2		R 3		R 4		R 1-4	
Time, s	2200.56		3474.94		2743.66		3629.82			
Microstrain	950	-950	990	-990	990	-990	990	-990	990	-990
Calculated	4.97	-4.97	5.15	-5.12	5.10	-5.10	5.10	-5.10	5.13	-5.13
3.5 Sigma	R 5		R 6		R 7		R 8		R 5-8	
Time, s	2749.02		3088.67		2242.29		1198.61			
Microstrain	990	-990	970	-950	970	-970	1010	-990	990	-990
Calculated	5.10	-5.10	5.03	-4.92	4.97	-4.97	5.10	-5.00	5.14	-5.08
2.5 Sigma	R 9		R 10		R 11		R 12		R 9-12	
Time, s	2686.84		1826.73		1842.24		3490.98			
Microstrain	990	-950	930	-930	870	-950	890	-910	990	-990
Calculated	5.03	-4.82	4.70	-4.70	4.39	-4.80	4.56	-4.56	5.03	-5.03

^aBlackglas beam, center strain gauge, channel 3.

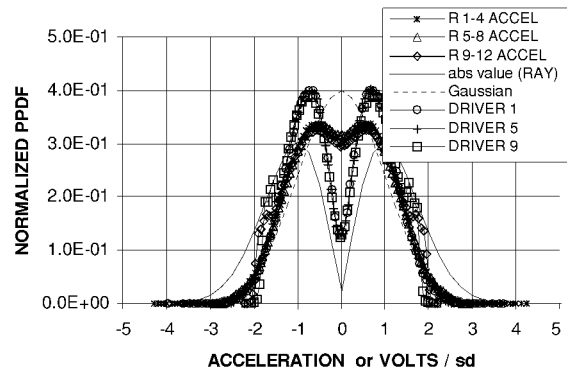


Fig. 9 Drive and accelerometer APDFs linear plots.

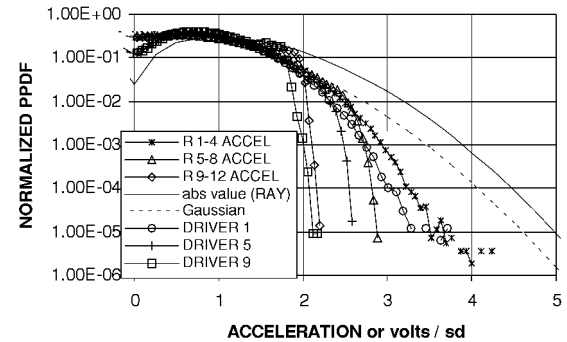


Fig. 10 Drive and accelerometer APDFs positive sigma log plots.

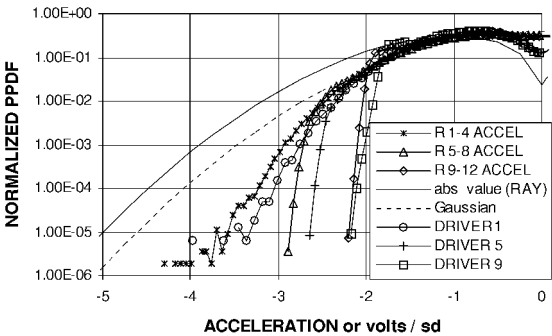


Fig. 11 Drive and accelerometer APDFs negative sigma log plots.

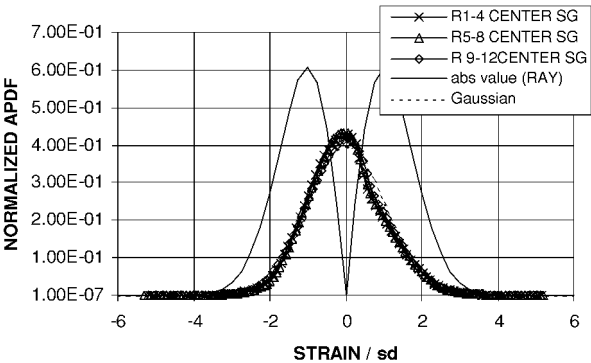


Fig. 12 Center strain gauge APDFs linear plots.

The highest and lowest sigma values obtained from the center strain gauge APDFs are listed in Table 2 for each of the four 4200-s records and for the combined 16,800-s records. With the sigma limited to 3.5, the maximum and minimum calculated sigma values for the first record were 5.10 and -5.10, indicating an increase in calculated sigma values. Some of the other records showed a decrease in calculated sigma values. The variability was limited to a range of positive values from 4.97 to 5.14 and negative values from -4.92 to -5.10. The combination of all four records was 5.14 and -5.08. The maximum and minimum calculated sigma value with sigma limited to 2.5 were lower than those calculated with sigma limiting off and sigma set at 3.5. The variability was limited to a range of positive values from 4.39 to 5.03 and negative values from -4.56 to -5.03. The sigma values calculated from the 4200-s records indicated a lowering in calculated sigma values as the controller sigma limiting value was increased. The peak strains from the combination records were equal to 990 microstrain. The effects on fatigue lifetimes can be estimated from the combination sigma value of 5.13 and 5.03. The resulting strains were 193.0 and 196.8 microstrain, or 193.0 is 98% of 196.8. The corresponding cycles-to-failure ratio was 70.7% using a sample room tempera-

ture Blackglas™ $\epsilon-N$ curve. The change in sigma values from 5.13 to 5.03 changed the cycles-to-failure and the time-to-failure to 29.3% of the higher strain value. A change of 0.10 in sigma values resulted in a reduction of 29.3% in the Blackglas coupon lifetime.

The center strain gauge APDFs were not symmetric about zero sigma, as shown in Fig. 12. They were shaped more nearly to the Gaussian distribution than the Rayleigh distribution. The log plots of the center strain gauge APDFs are shown in Figs. 13 and 14. Both the sigma turned off and the 2.5 sigma limiting tests were Gaussian. The tails of the 3.5 sigma limiting tests showed smaller amplitudes on the ends of the curves. Similar results were found with the side strain gauge. The side strain gauge APDFs are shown in Fig. 15. These were similar to the center strain gauge APDFs except the APDFs peak at 0.37, whereas the center strain gauge APDFs peak at 0.42. The displacement APDFs are shown in Fig. 16. The APDFs of the narrowband and wideband processes are theoretically that of a Gaussian shape. These tests were conducted with a narrowband random excitation. The shapes of all of the APDFs were a Gaussian distribution as expected; however, the shapes were considered non-Gaussian.

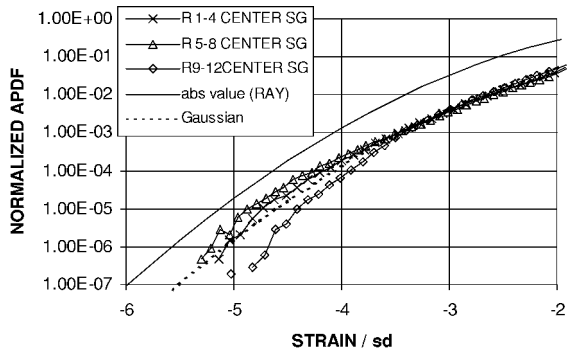


Fig. 13 Center strain gauge APDFs negative sigma log plots.

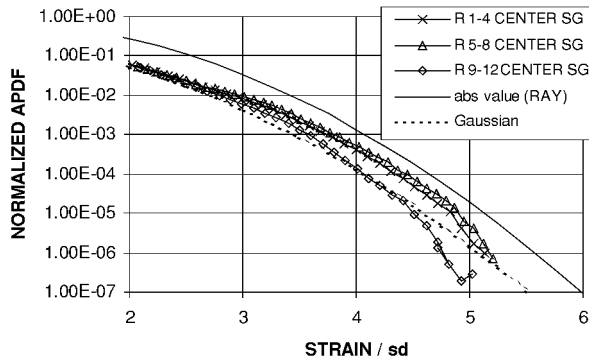


Fig. 14 Center strain gauge APDFs positive sigma log plots.

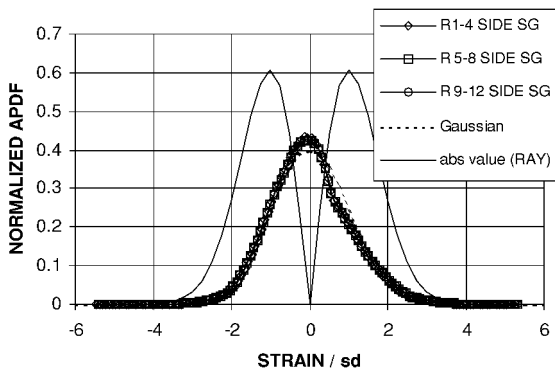


Fig. 15 Side strain gauge APDFs linear plots.

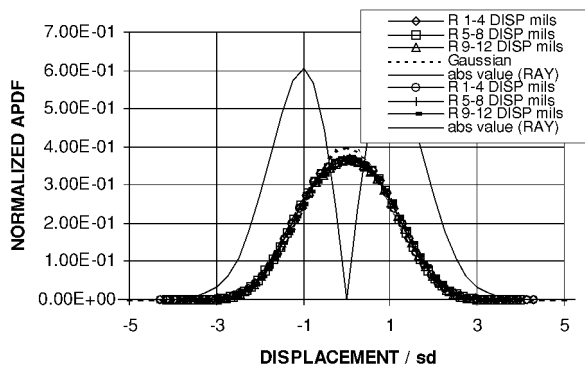


Fig. 16 Displacement APDFs linear plots.

The next two paragraphs discuss PPDFs. All of the peaks were counted by including all that have a zero slope in their time histories. The PPDFs for the drive signal and the accelerometer are shown in Figs. 17–19. The drive signal and the accelerometer PPDF shapes changed around zero sigma. The drive signal PPDFs were shaped more like a Rayleigh distribution. The shape of the drive and accelerometer PPDF for 3.5 sigma did not fit a smooth function around ± 1.60 and ± 1.75 ma. Some distortion was noted for

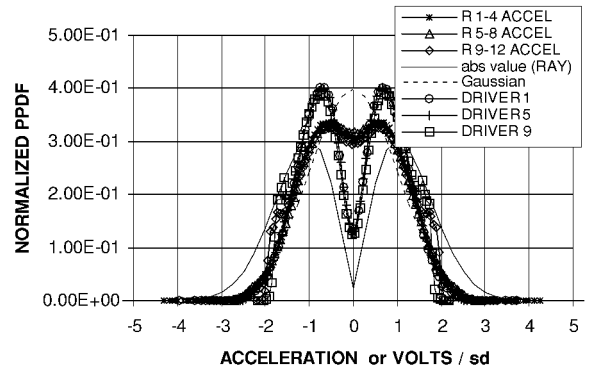


Fig. 17 Drive and accelerometer PPDFs linear plots.

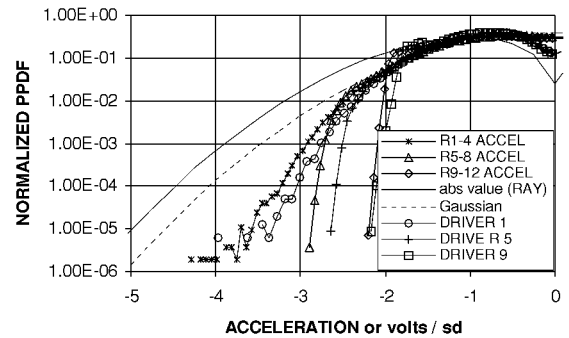


Fig. 18 Drive and accelerometer PPDFs negative sigma log plots.

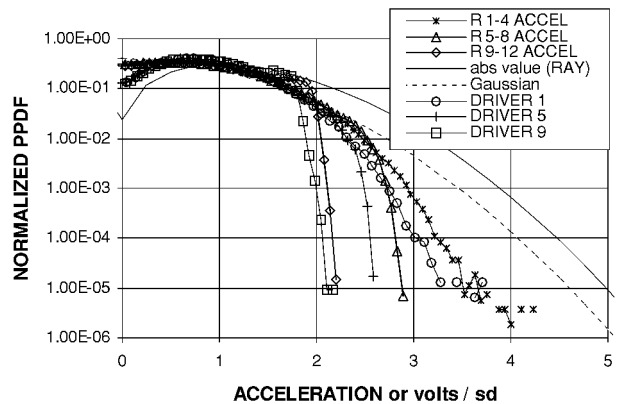


Fig. 19 Drive and accelerometer PPDFs positive sigma log plots.

the heavy clipping of the input signals. This was not the case in the output signals.

The PPDFs for the center strain gauge are shown in Figs. 20–22. The negative side of the PPDFs peaked at a higher PPDF value than the positive side. Sigma limiting reduced the sigma value from -3.5 to -2.0 in the tails of the curves. The positive side clipping did not have as much effect on the shape of the PPDF as that observed for the negative side. Similar results were obtained with the side strain gauge signals. However, the tails showed a spread in the positive and negative values from the sigma limiting turned off to 2.5 and 3.5 sigma clipping. The results indicated that higher sigma limiting values resulted in lower sigma values, but the magnitudes were higher for the higher clipping tests. Also noted were changes in the rms values and the SD values, which in turn lower the calculated sigma values.

With the vibrometer measurements, the ranges of maximum and minimum calculated values from the PPDFs for all test conditions were from -4.13 to -4.29 and from 4.29 to 4.02 . The maximum and minimum calculated sigma values were smaller for the 3.5 sigma limit test (test 3) than the test with the sigma limiting off (test 1). The PPDFs for the displacements are shown in Figs. 23–25. The

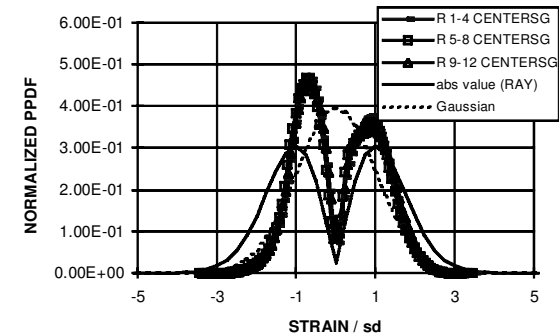


Fig. 20 Center strain gauge PPDFs linear plots.

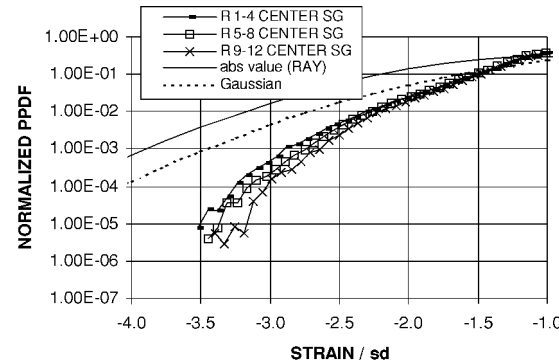


Fig. 21 Center strain gauge PPDFs negative log sigma.

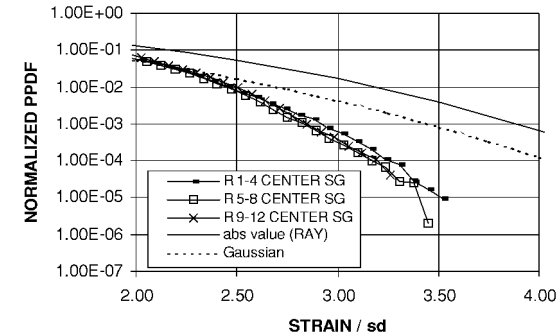


Fig. 22 Center strain gauge PPDFs positive sigma log plots.

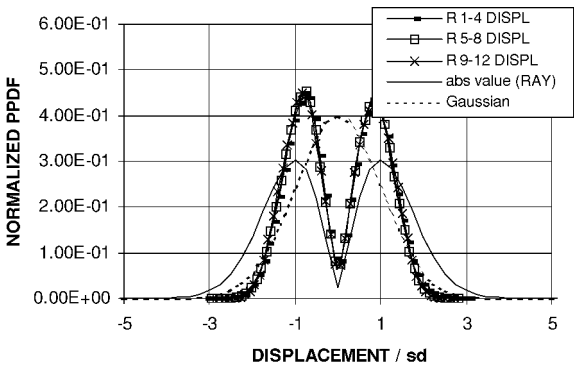


Fig. 23 Displacement PPDFs linear sigma log plots.

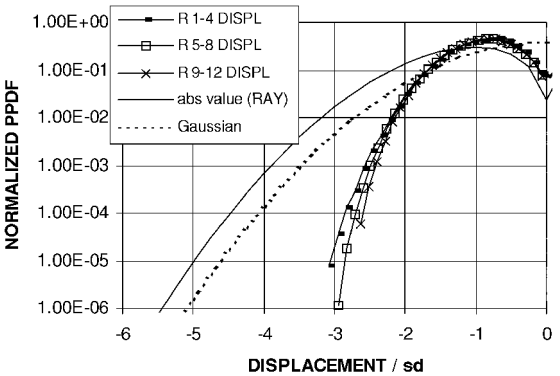


Fig. 24 Displacement PPDFs negative sigma log plots.

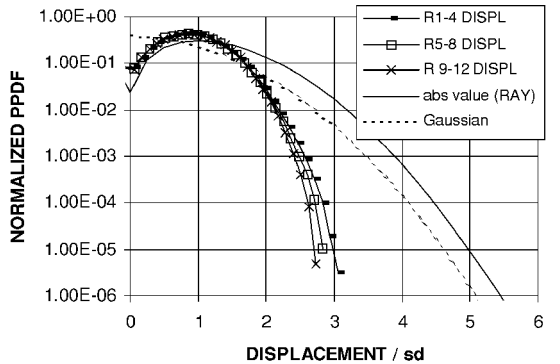


Fig. 25 Displacement PPDFs positive sigma log plots.

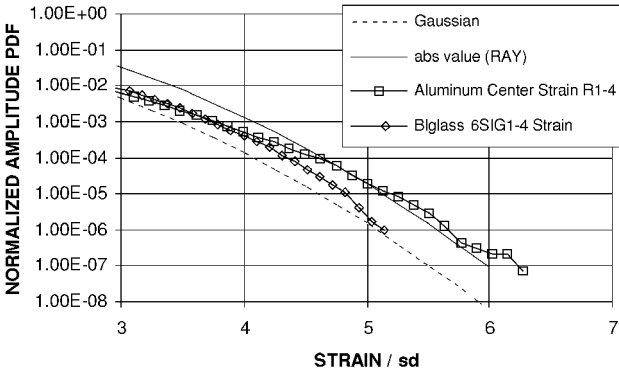


Fig. 26 Blackglas and aluminum alloy positive APDFs comparison.

PPDFs were approximately symmetric. Similar results were found with the tails of the curves of the displacement PPDFs. Sigma limiting reduced the calculated sigma values slightly. The PPDFs of a narrowband process are theoretically that of a Rayleigh distribution. The shapes of all of the PPDFs were close to a Rayleigh distribution as expected because the tests were conducted with a narrowband random excitation; however, the shapes are considered non-Rayleigh.

The Blackglas center strain gauges' APDFs were compared with similar tests with an aluminum alloy beam center strain gauge.¹ Comparisons between Blackglas and aluminum alloy coupons are shown in Figs. 26 and 27. The largest negative value for the aluminum coupon was -5.76 and for the Blackglas coupon -5.13 . The largest positive value for the aluminum coupon was 6.27 and for the Blackglas coupon was 5.14 . The Blackglas coupon tails were symmetric and closer to a Gaussian than a Rayleigh distribution. Sufficient time was allowed for a six sigma event; however, the highest sigma event was 5.14 with the center strain gauge. The higher values from the aluminum coupon tests can be attributed to higher damping in the Blackglas coupon.

The PPDFs are needed in computing the damage accumulation using Miner's rule to predict sonic fatigue lifetimes.² This is accomplished by determining the number of peaks from the time history over the full range of amplitudes, along with Miner's rule² and an $\epsilon-N$ curve for Blackglas. The normalized high-cycle fatigue damage shown in Fig. 28 was computed as a function of the sigma values measured.

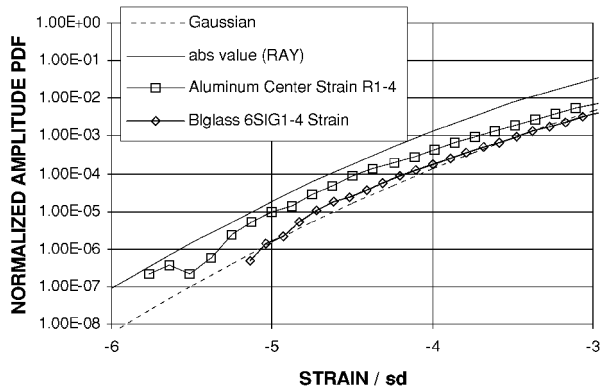


Fig. 27 Blackglas and aluminum alloy negative sigma APDFs comparison.

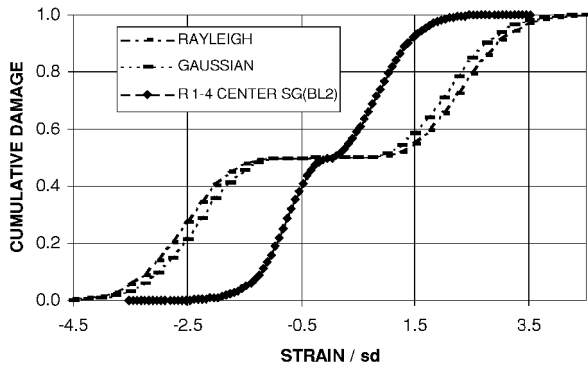


Fig. 28 Blackglas center strain gauge runs 1-4 cumulative damage curve.

More damage per peak is accumulated at the higher sigma values, which have larger amplitudes; however the larger peaks only account for about 5% of the damage. The remaining damage occurred between -1.70 and -0.30 sigma and between 0.30 and 1.70 sigma. There were only five peaks at -3.52 sigma and four at 3.52 sigma out of over 7×10^6 peaks measured. No damage occurs at zero sigma. Little damage accumulated around the tails of the curve due to the small number of peaks involved compared with the total number.

Conclusions

The APDFs of the narrowband are theoretically that of a Gaussian distribution. These tests were conducted with a narrowband random excitation. The shapes of all the APDFs calculated were more nearly the shape of a Gaussian distribution as expected. However, the shapes were considered non-Gaussian due to the lack of symmetry and the differences between the measured values and the Gaussian values. The PPDFs of a narrowband process are theoretically that of a Rayleigh distribution. The shapes of all of the PPDFs were close to a Rayleigh distribution as expected; however, the shapes were considered non-Rayleigh due to the differences between the measured and the Rayleigh distribution.

Clipping the peaks usually reduces the rms level. However, in these tests the rms level was kept at a constant 200 microstrain for comparison purposes. This resulted in many more peaks in the input signal closer to 3.5 and 2.5 sigma values than those with the sigma limiting turned off. The highest sigma values of the drive signal occurred with the sigma limiting turned off. The peak center strain gauge and displacements sigma values were reduced when the sigma limiting was turned on. A change in sigma values of 0.10 from the sigma off to the 2.5 sigma limiting test condition in the 16,800 s of strain response signals resulted in a reduction of calculated 29.3% in the Blackglas coupon lifetime. This amount of change or more also occurred in the comparisons of the records from one 4200-s time sample to the next 4200 sample. The duration of both time samples did not include enough samples to reduce the variability in the SD or the rms strain and vibrometer values. Some variability occurred when all of the 16,800 s of data was used. This shows that the data changed significantly with time, which also means that the data were not truly stationary. To define the shape of the PPDFs 1-h records were sufficient, but not the rms or other statistical properties. Further studies are needed to determine the effects of record length on the statistical properties of the input and the response signals. Also further studies are recommended to determine the effects of clipping of the input and the response signals on the statistical properties of both.

References

- ¹Wolfe, H. F., Camden, M. P., Brown, D. L., and Simmons, L. M., "Six Sigma Effects on the Response of a Cantilevered Beam with Random Excitation," *Proceedings of the 67th Shock and Vibration Symposium*, Nov. 1996.
- ²Miner, M. A., "Cumulative Damage in Fatigue," *Journal of Applied Mechanics*, Vol. 12, 1945, pp. A159-A164.